17th World Conference on Earthquake Engineering, 17WCEE
Sendai, Japan - September 13th to 18th 2020

TOPOGRAPHY OF QUATERNARY SEDIMENTS IN KATHMANDU BASIN FROM ARRAY MICROTREMOR OBSERVATIONS

N. Poovarodom[(1)], A. Jirasakjamroonsri [(2)], D. Chamlagain[(3)], P. Warnitchai[(4)]

[(1)] *Associate Professor, Dept. of Civil Engineering, Thammasat University, Thailand, pnakhorn@engr.tu.ac.th*
[(2)] *Postdoctoral Fellow, Dept. of Civil Engineering, Thammasat University, Thailand, amorntep_aj@hotmail.com*
[(3)] *Assistant Professor, Department of Geology, Tri-Chandra M. Campus, Tribhuvan University, Nepal, deepakchamlagain73@gmail.com*
[(4)] *Professor, School of Engineering and Technology, Asian Institute of Technology, Thailand, pennung.ait@gmail.com*

Kathmandu, Nepal, is located in the intermontane basin which is bounded by out of sequence thrust to the north and Chandragiri Fault to the south. This area is highly vulnerable to earthquake due to the active tectonics and local fragile geological conditions. Subsoil beneath Kathmandu can be characterized by the Quaternary lacustrine sediments with variation depth of basement rock, however spatial variation and details of sediments are very limited for evaluation of the seismic site effects. The horizontal components of the ground motion during the main shock of the 2015 earthquake exhibit dominant period in the range of about 4 to 5 second. These unusual long period waves could possibly be resulted from effects of thick and soft sediments. Although the site effects have long been recognized, past researches for this issue in Kathmandu valley are quite primitive. Therefore, the objective of this study is to explore the site conditions of the area especially at deep level to understand the basement topography using array microtremor observations. Altogether 30 sites, which are distributed across the valley, are explored. The Centerless Circular Array (CCA) technique is employed to determine phase velocity, and inversion analysis is used to compute the shear wave velocity profile down to basement rock. The arrangement of the microtremor sensors was an equilateral triangular array and different sizes of array were set with radius from 1 to 120 m dependent on site conditions. The observed phase velocity dispersion curves can provide long detectable wavelength and sufficient accuracy for inversion analysis of shear wave velocity profile of sedimentary sites down to 500 m or deeper. The depths of basement underneath the Quaternary lacustrine sediments can be identified from the level with shear wave velocity greater than 2,000 m/s. The inferred depth of basement ranges from few meters at rock outcrop or basin edge to about 600 m in the central area of the basin. The topography of the Quaternary sediments derived by this study is in good agreement with the results from the gravity survey where the thickness of the Quaternary sediments was calculated based on the assumed density difference of 0.8 g/cm^3 between the layers. Finally, site transfer function for all observation sites was computed and the predominant frequency at the sites was considered to propose a seismic microzonation map of the basin.

Keywords: Site effects; Deep Quaternary sediments; Shear wave velocity; Array microtremor; Kathmandu

1. Introduction

Kathmandu valley, Nepal, is located in the intermontane basin, which is highly vulnerable to earthquake due to the active tectonics and local fragile geological conditions. The city suffered from many destructive earthquakes in the past, e.g. earthquake of 1255, 1408, 1681, 1803, 1810, 1833, 1866, 1934, and 1988. The most recent April 25, 2015 Mw7.8 Gorkha earthquake caused massive damages in Kathmandu Valley, causing more than 8,000 casualties and injuring more than 22,000 people [1]. The horizontal components of the ground motion during the main shock of this earthquake recorded on sedimentary site exhibit dominant period component in the range of about 4 to 5 second whereas those on a rock site was dominant at short period [2]. This unusual long period wave possibly indicates the site effects caused by thick soil layer with a thickness of up to several hundred meters. Moreover, the distributions of damage caused by this event were observed to be non-uniform. Therefore, seismic site effects in Kathmandu valley are very important issues to be studied in order to mitigate the seismic risk in the area.

The effects of soil sediments on ground motion characteristics have long been recognized, however, past research studies for this area are still quite primitive. Subsoil beneath Kathmandu can be characterized by the soft fluvio-lacustrine sediments with variation depth of basement rock, however spatial variation and details of sediments are very limited for evaluation of the seismic site effects. Since there is lacking of understanding of the subsoils structure especially at deeper level, this research aims to explore such information for Kathmandu valley and investigate the amplification characteristics resulted from the seismic site effects. The economical means of array microtremor observation employed in the study is the Centerless Circular Array (CCA) technique. Altogether 30 sites are explored for shear wave velocity profile down to basement rock. The depth of the interface between the Quaternary lacustrine sediments and the basement rock is derived from the shear wave velocity profile. The obtained topography of the Quaternary sediments from this study is compared and discussed with the gravity surveys from a previous research. The site transfer functions were computed from the derived velocity structures and their spatial variations were considered for seismic microzonation of the basin.

2. Area of study

The intermontane basin of Kathmandu lies on the large crystalline thrust sheet, which consists of low to medium grade metamorphic rocks and overlying fossiliferous sedimentary sequence of Tethyan sediments [3]. The Kathmandu valley is bounded by out of sequence thrust to the north and Chandragiri Fault to the south. The structural data have revealed a bowl shaped basin in the valley with varying depth and isolated bedrock hillocks scattered in the basin. Basement topography of the valley was investigated by gravity survey [4]. The interface of the Quaternary sediments and the Paleozoic basement meta-sediments was identified based on the observed density difference of 0.8 g/cm^3. The maximum basement depth was estimated to be about 650 m around the central of the basin.

The area of study is located within latitudes 27°37’ N to 27°47’ N and longitudes 85°15’ E to 85°25’ E, covering Kathmandu and the neighboring municipalities. Altogether 30 sites of microtremor observation sites were selected and distributed in the basin. Fig. 1 shows the area of study and distribution of observation sites, which is shown by number and marker classified into different groups. The meaning of each marker is given in the discussion of the results.

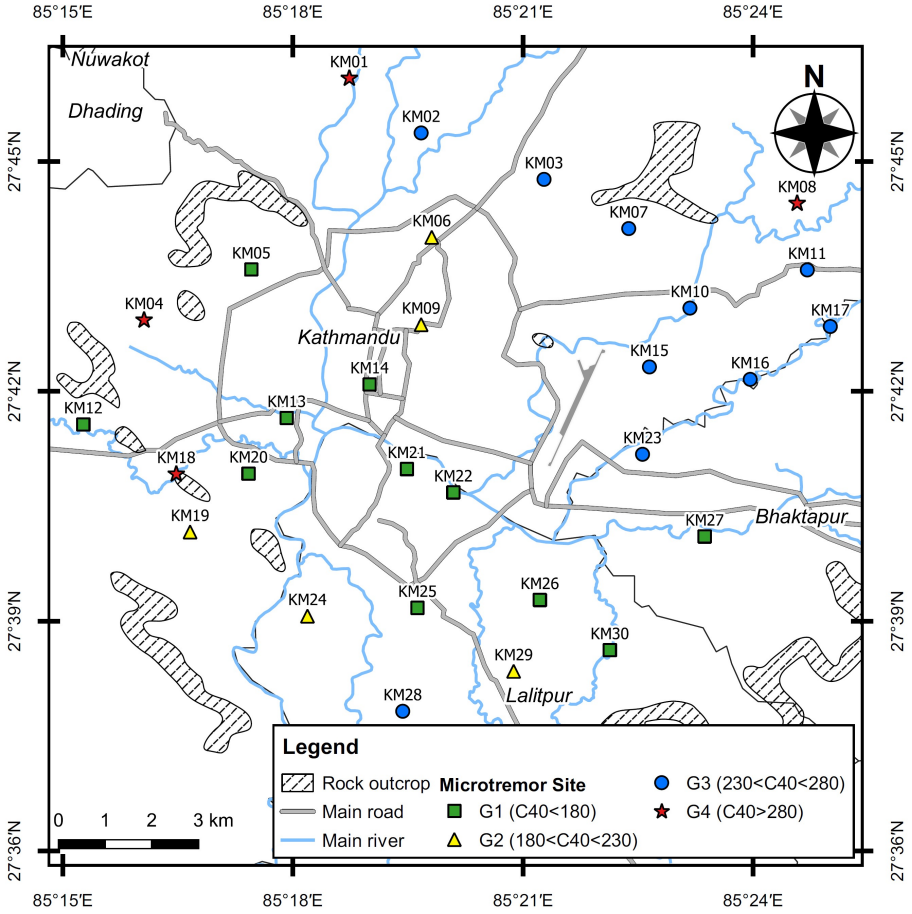

Fig. 1 –Area of study and microtremor observation sites

3. Method of study; Microtremor observation

3.1 Centerless Circular Array (CCA) method

The technique to process microtremor data used in this study is the Centerless Circular Array (CCA) method. This technique was developed by Cho et al. (2006) [5] based on spectral ratio representations. The spectral ratio which contains information of phase velocities is an integration of all information on the field of vertical component of microtremor. Field works require to deploy a circular array of radius r and record the vertical component of microtremor $z(t,r,\theta)$. Define the average value $Z_0(t,r)$ along the circumference and its weighted average $Z_1(t,r)$ as;

$$Z_0(t,r) = \int_{-\pi}^{\pi} z(t,r,\theta)d\theta \tag{1}$$

$$Z_1(t,r) = \int_{-\pi}^{\pi} z(t,r,\theta)\exp(i\theta)d\theta \tag{2}$$

Assuming that the fundamental Rayleigh wave mode dominates the vertical component of the microtremor field, the ratio of their power spectra densities, $G_0(r,r;\omega)$ and $G_1(r,r;\omega)$, can be written as;

$$\frac{G_0(r,r;\omega)}{G_1(r,r;\omega)} = \frac{J_0^2(rk(\omega))}{J_1^2(rk(\omega))} \tag{3}$$

Where J_0 and J_1 is the Bessel function of the first kind with the zero-th order and the first order, respectively. The wavenumber *k(ω)* and phase velocity *c(ω)*, are then estimated by fitting the observed spectral ratio (the left-hand side term of Eq. 3) with a theoretical ratio (the right-hand side term of Eq. 3). The above statement holds in noise-free conditions, where noise is considered as the non-propagating components contained in the field of microtremors. In general practice which noise is contained, equation (4), for the case of the fundamental mode dominating, can be shown as;

$$\frac{G_0(r,r;\omega)}{G_1(r,r;\omega)} = \frac{J_0^2(rk(\omega))+\varepsilon(\omega)/N}{J_1^2(rk(\omega))+\varepsilon(\omega)/N} \tag{4}$$

ε is the noise-to-signal ratio and N is the number of seismometers placed around the perimeter. The wavenumber k, and phase velocity c, are then estimated by fitting the observed spectral ratio with the right-hand side term of equation (4).

3.2 Instrument and Field observation

The instrument used for microtremor observation consists of velocity sensors that can measure in the frequency range of 0.1 to 70 Hz connected to the receivers and converted to the digital signal. The sensors used are 4 sets, each set measured simultaneously with the time synchronization using a clock from the GPS with a resolution of 1 /100 seconds.

Before conducting array microtremor observation, a test was performed to check the coherency of amplitudes and phase differences among the sensors by placing them closely next to each other and comparing their signals. The applicable range of frequency for the equipment was identified as from 0.3 to 50 Hz. The array configuration is equilateral triangular array network. Three sets of sensors are placed at the corners of a triangle (or a circle), and one at the centre. Different sized array arrangements were set at each site with radius ranging from 5 to 120 m for thick sedimentary sites and from 1 to 30 m for shallow sedimentary sites. The duration for collecting vibration data is about 40 minutes for each array. Fig. 2(a) shows the arrangement of the vibration sensors for the coherency check and Fig. 2(b) for an equilateral triangular array.

3.3 Analysis of Microtremor Data and Inversion Analysis

The first result from CCA is the observed spectral ratio as shown on the left-hand side of Eq. (4) and it is then compared to the ratio of Bessel function on the right-hand side of Eq. (4). By fitting the two functions, the identified f_i and rk_i can be obtained. Phase velocities are then computed by $c_i = 2\pi f_i / k_i$. The dispersive characteristics of phase velocity and frequency can be consequently obtained from their ensemble for different arrays. From the dispersion relation of phase velocity and frequency, the results from field observations were then compared with those derived theoretically from a horizontally layered earth model by iteration procedure. The results of best-fit shear wave velocity–depth profile were determined from the inversion analysis. This study employs two algorithm for inversion analysis; the combination of Down Hill Simplex Method with Very Fast Simulated Annealing [6] and the neighbourhood algorithm [7].

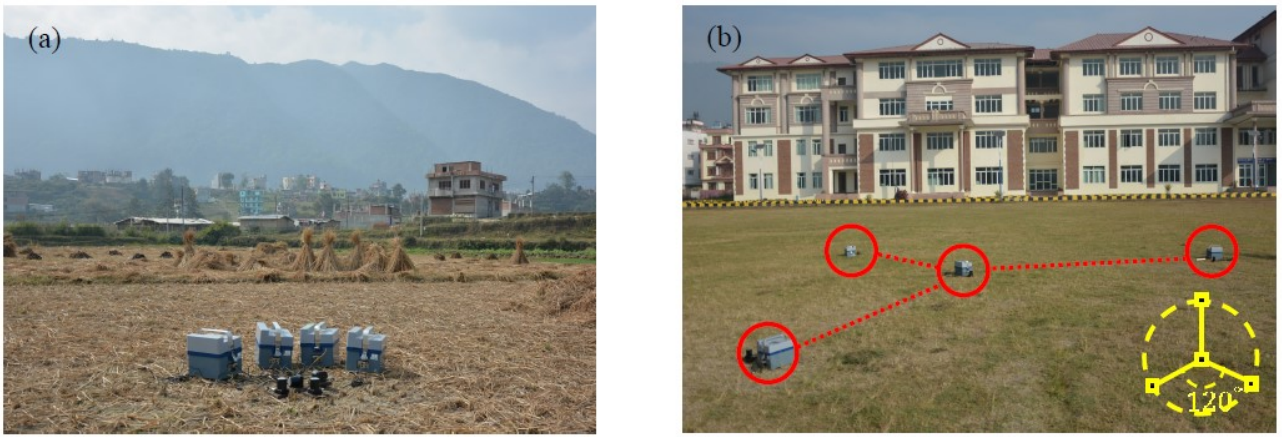

Fig. 2 – Arrangement of vibration sensors (a) coherency check, and (b) an equilateral triangular array.

4. Results and Discussions

4.1 Phase Velocity Dispersion Curve

The derived phase velocity dispersion curves from the microtremor observations are presented in this section. To clarify the presentation and discussion, the results from 30 sites are classified into four groups based on the value of the phase velocity at wavelength of 40 m (C_{40}). This value was shown to be a simple estimation of the average shear wave velocity to a depth of 30 m (Vs_{30}) [8]. In the following discussion, each group consists of sites having C_{40} as follows; C_{40} is less than 180 m/s in the group G1, $180 < C_{40} < 230$ m/s in G2, $230 < C_{40} < 280$ m/s in G3 and is C_{40} greater than 280 m/s in the group G4.

The locations for the sites in the groups are also presented in Fig. 1 with different markers described in the legends of the map. Generally, soft sedimentary sites yield low shear wave velocity or low phase velocity, and vice versa. The locations of the sites of low C_{40} in G1 are in the central area, this observation implies that the area of this group is underlain by soft sediments. Areas with higher phase velocity in G2 and G3 are spread out from the central area, respectively. Hill sites on the northern basin boundary or a rock outcrop site are characterized by their relatively high phase velocity and classified in G4.

The results of phase velocities of the 30 observation sites are plotted versus periods in Fig. 3(a) to (d) for G1 to G4, respectively. It can be noted that large variations exist, indicating remarkable differences of site characteristics inside the study area. Since waves propagating with long period possess long wavelength and they travel at deeper level from surface, dispersion curves of low phase velocity at long period represent the waves travel with low velocity (in soft media) deeply beneath the surface. Then the sites having gentle slope-dispersion curves of phase velocity-period, Fig. 3 (a) and follows by Fig. 3 (b), lie on soft soil. Those sites are located at the central area of study. For the sites having steep dispersion curves of phase velocity-period, Fig. 3 (c) and (d), lie on much stiffer soil. Those sites are located near the boundary of the study area or near rock outcrop.

The derived phase velocity dispersion curves from the observation at sedimentary sites provide long detectable wavelength and sufficient accuracy for inversion of shear wave velocity profile down to 500-1,000 m, whereas at some stiff soil sites in G4 exhibit shorter detectable wavelength. The depths of basement were clearly identified from the level with shear wave velocity greater than 2,000 m/s as the sample shown in Fig. 4. The inverse value of phase velocities (slowness) in Fig. 4(a) from field observations are compared with those derived theoretically from a horizontal layered model by iteration procedures to provide the best-fit shear wave velocity profile by the neighborhood algorithm as shown in Fig. 4(b). The results of Vs profile of all sites are presented in Fig. 4(c).

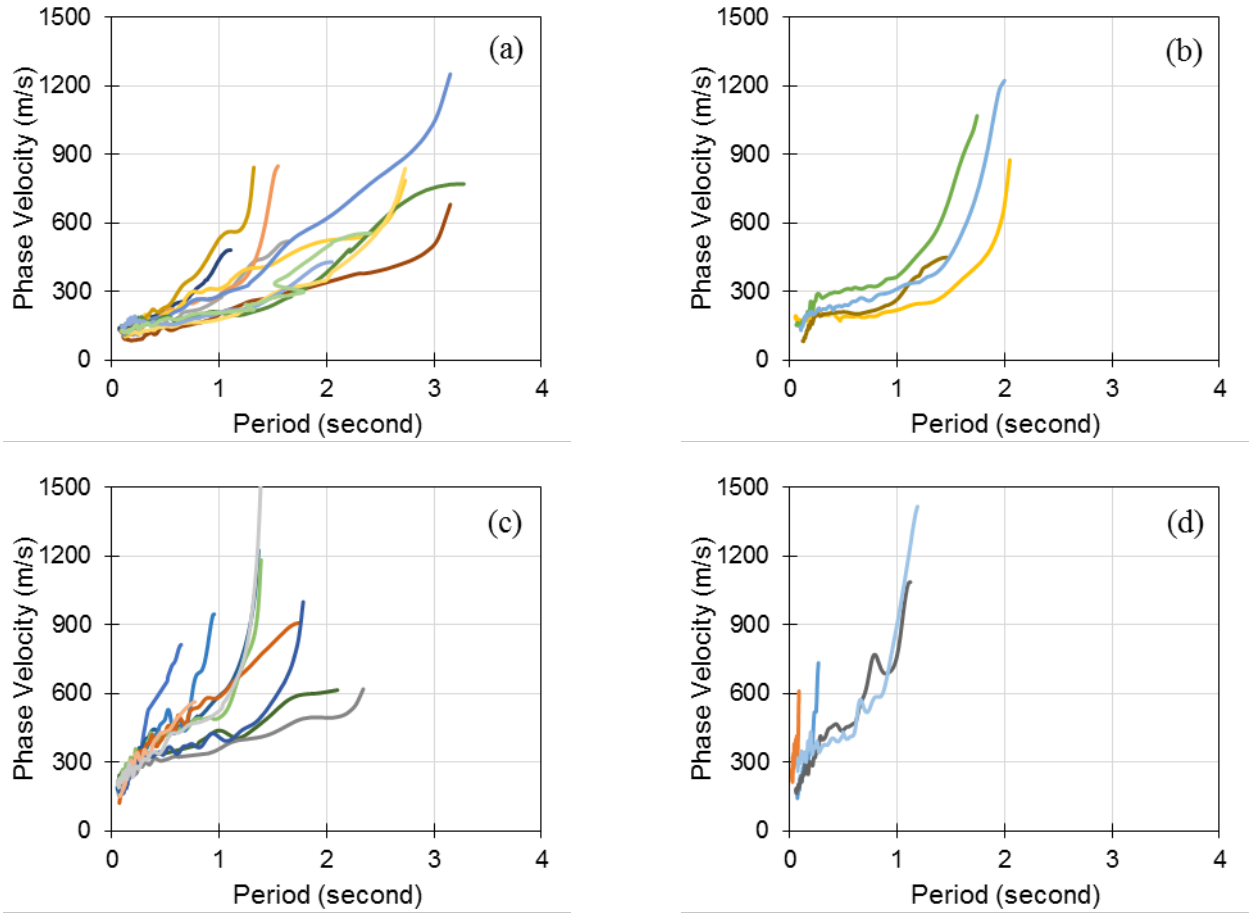

Fig 3 – Phase velocity-period dispersion curves (a) G1, (b) G2, (c) G3, and (d) G4

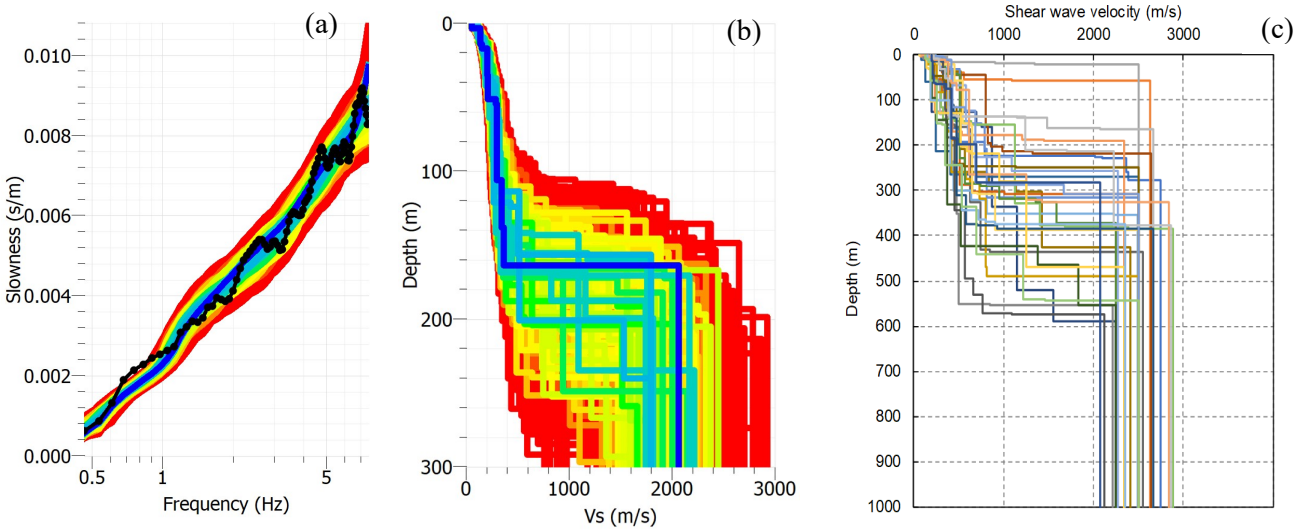

Fig. 4 – Inversion analysis of phase velocity dispersion curve (a) slowness, (b) result of an inversion analysis, and (c) Vs profile of all sites

4.2 Basement Topography

From the derived shear wave velocity profiles from all sites, the level of high contrast in velocity where Vs is greater than 2,000 m/s is inferred as the interface of the Quaternary lacustrine sediments over the basement rock. Then the topography of the basement underneath the Quaternary lacustrine sediments can be drawn from that depth. As shown in Fig. 4 (c), the depth of basement ranges from few meters for sites which are located on rock outcrop or mountain hills to about 600 m in the central area of the valley. The existent variation the basement depth can be illustrated as a colored-contour map in Fig. 5. The central area of the basin shows the maximum depth of basement, whereas the basement is very shallow at the rock outcrop area on the western part of the studied area. The basement topography derived in this study is then compared with the results from the gravity survey in a previous study [4], where the boundary of the Quaternary sediments and the Paleozoic metasediments was estimated based on the assumed density difference of the two-layer structure model of 0.8 g/cm^3. Fig. 5 includes the comparison between these studies, where the results from gravity survey are plotted as dotted contour lines. For more detailed comparisons, four cross sections across the valley are made and their alignment are shown as colored lines in Fig. 5. The plots of the 2D basement topography along these sections are shown in Fig. 6 (a) to (d). Generally, the comparisons of both studies are mostly in good agreement for all locations. Some discrepancies exist that could be attributed to the variability of the sediments resulted from distance between the sites from both investigations.

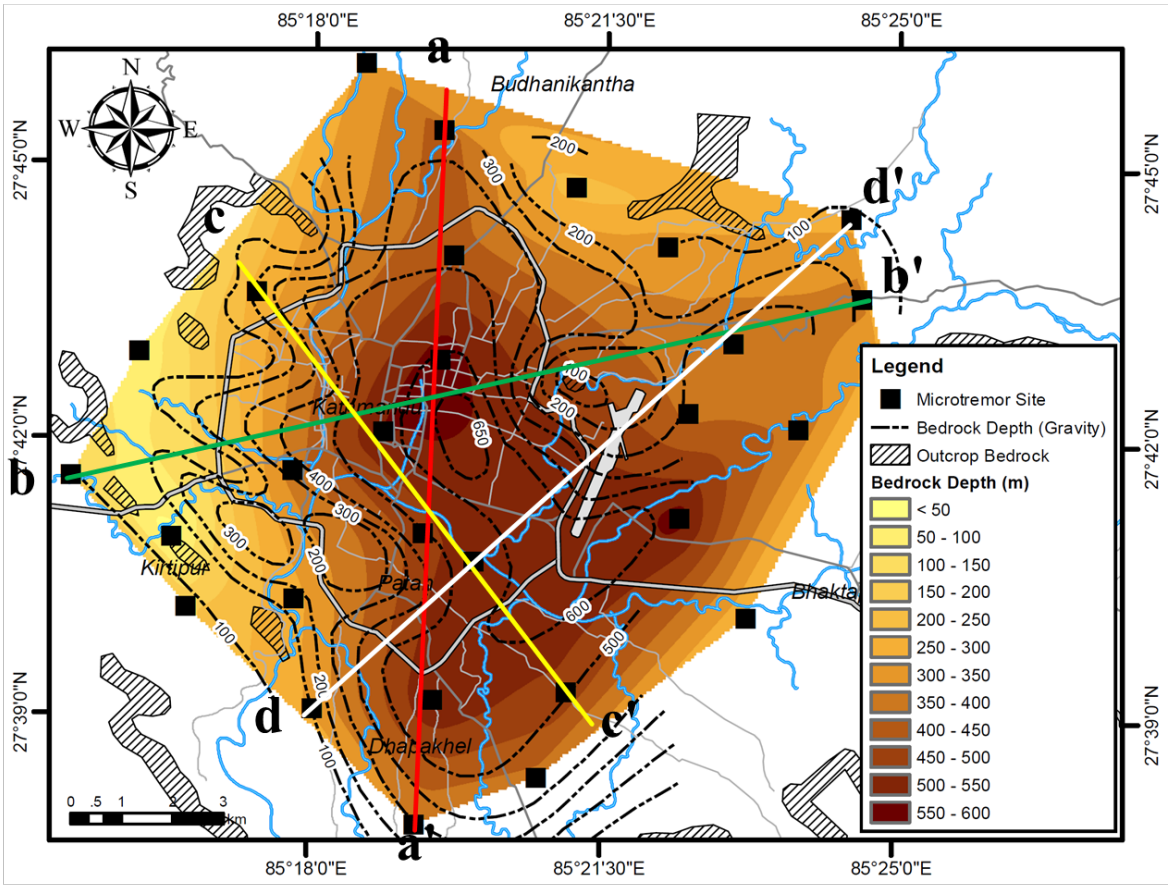

Fig. 5 – Map of basement depth of Kathmandu valley

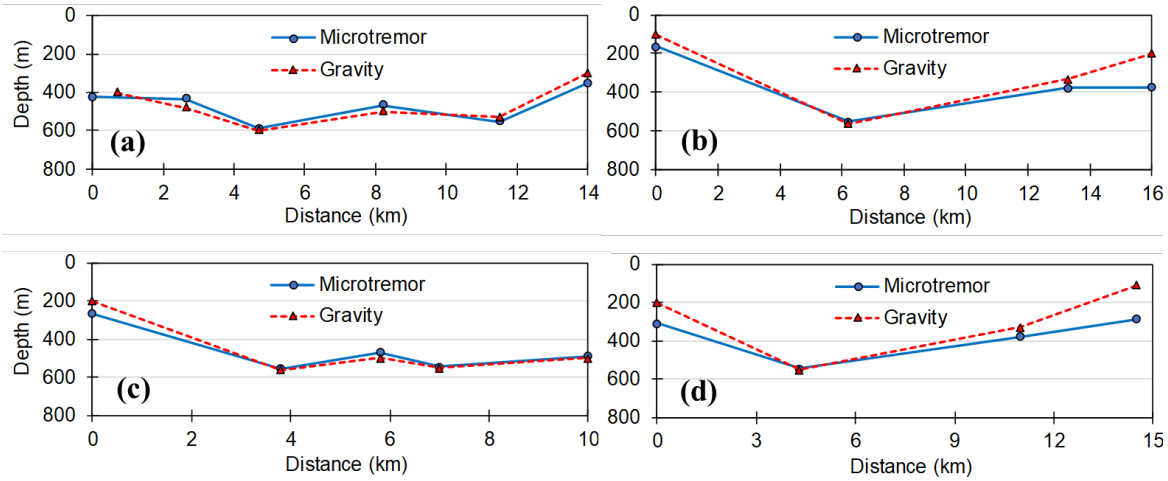

Fig. 6 – 2D Cross section for comparison of basement topography from this study and gravity survey

4.3 Transfer Functions

From the computed shear wave velocity structures, soil layers of each site were modelled for site response analysis to investigate their amplification characteristics. Transfer functions of vertical propagation of wave were analyzed by one dimensional analysis using SHAKE [9]. Damping ratio was assumed to be 5% of the critical value. The results of all sites are used to sub-divide the studied area into four zones based on the site frequency of the fundamental mode or the predominant frequency. Zone 1 to zone 4 represent sites having the predominant frequency lower than 0.33 Hz, 0.33 to 0.50 Hz, 0.50 to 1.0 Hz, and higher than 1.00 Hz respectively. Fig. 7 (a) to (d) show the plots of the transfer functions in these zones.

This results indicate that the predominant frequency from site transfer functions at the center of Kathmandu valley is lower than 0.33 Hz (or the predominant period is longer than 3 second), and the predominant frequency increases for the area located apart from this area. The northern and western part of this study exhibit the predominant frequency higher than 1.00 Hz. where these areas are located at the boundary of the basin or rock outcrop. The spatial variation of the predominant frequency could lead to the seismic microzonation map of Fig. 8. The central area of the basin shows potential amplification at low frequency component of ground motion. The amplifications in this area indicate a risk of amplified ground motions which can resonate with tall buildings having natural frequency in this range. The area of the boundary of the basin in the north and a rock outcrop in the west show amplification at high frequency.

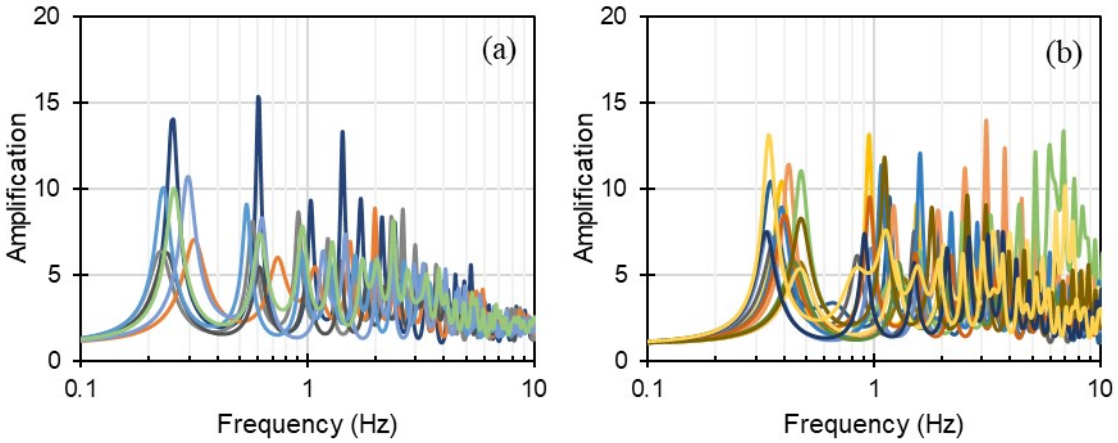

Fig 7. – Transfer function (a) zone 1, (b) zone 2, (c) zone 3, and (d) zone 4

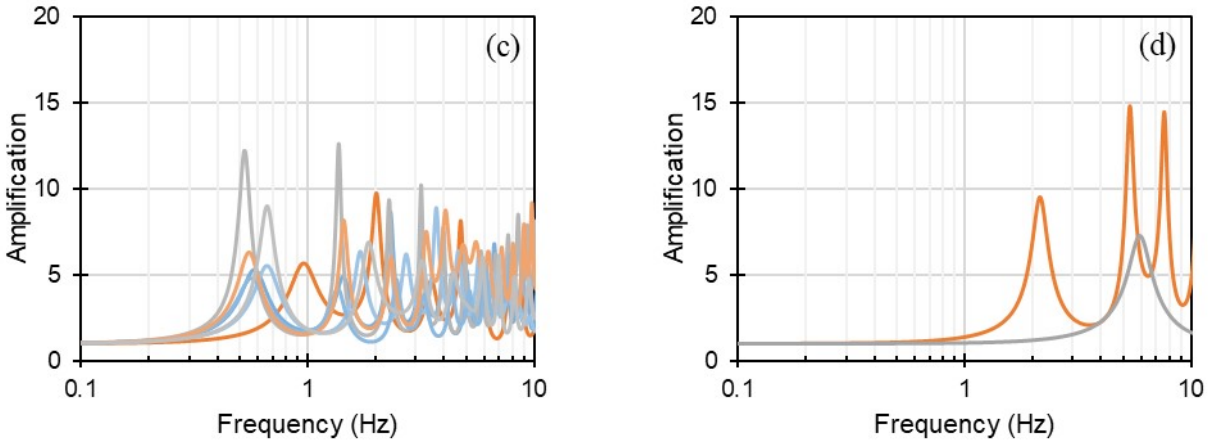

Fig 7. (cont.) – Transfer function (a) zone 1, (b) zone 2, (c) zone 3, and (d) zone 4

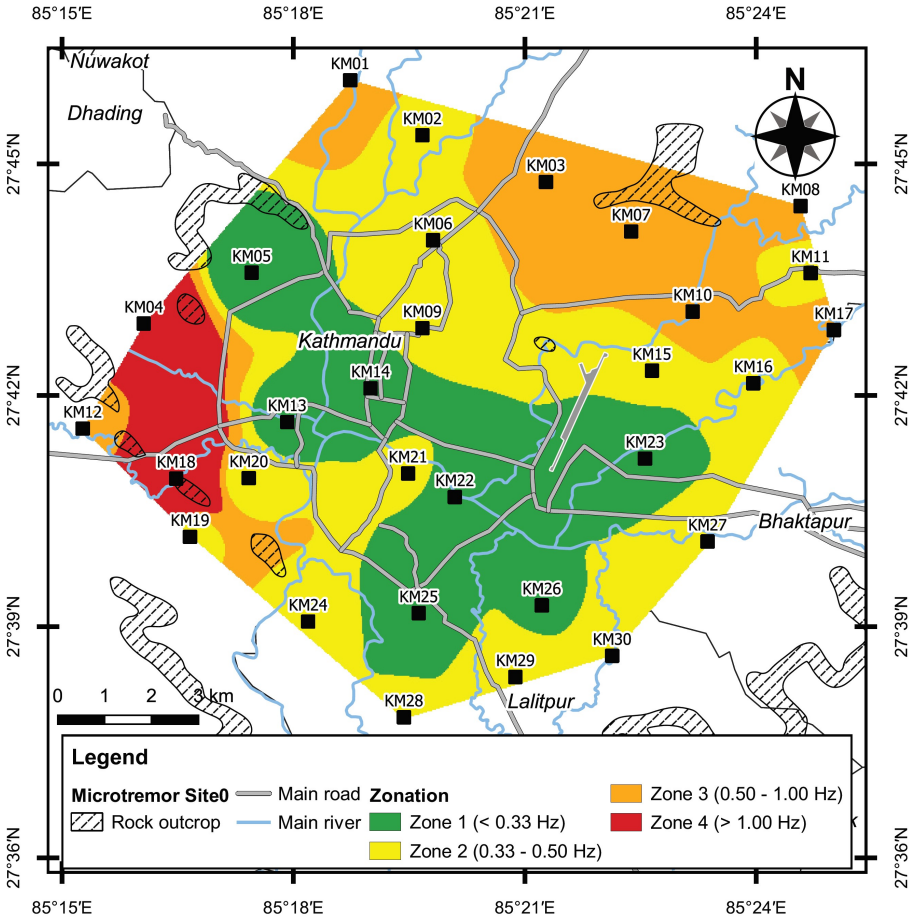

Fig. 8 – Seismic zonation map of Kathmandu valley from site transfer function

5. Concluding Remarks

This article presents results from microtremor observation and site response analysis of Kathmandu valley which has substantial risks of strong earthquake and site amplification from the soft sedimentary deposits in the basin. Shear wave velocity profiles of 30 sites across the basin were explored by the Centerless Circular Array (CCA) microtremor observation technique. The basement topography was derived from spatial variations of the depth of the Quaternary lacustrine sediments which were identified from the level with shear wave velocity greater than 2,000 m/s. Cross sectional profiles along north to south and west to east of the study area were presented to depict the shape of the basin underneath the sediments. The estimated depth of bedrock varies from few to about 600 meters. The boundary of the basin possesses shallower depth of bedrock comparing with the central area of the basin. The topography of the Quaternary sediments derived by this study is in good agreement with the results from gravity survey. Transfer functions obtained from site response analysis show amplifications in wide range of periods. A seismic microzonation map was presented based on the predominant frequency. Site amplification at long period could be pronounced in the central area whereas short period amplification could be anticipated at the basin boundary and rock outcrop sites. This finding is comparable to the observation from the 2015 Gorkha earthquake as the records on sedimentary sites were of long-period, high-velocity type comparing with those on rock sites nearby.

6. Acknowledgements

This study is supported by the Thailand Research Fund, research number RDG5630018 and Faculty of Engineering, Thammasat University. The authors are thankful to Mr. Weera Choopthong, Mr. Dipendra Gautam and Mr. Bibek Giri for their support during fieldwork.

7. References

[1] GEER (2015): Geotechnical field reconnaissance: Gorkha (Nepal) earthquake of April 25 2015 and related shaking sequence. *Geotechnical Extreme Event Reconnaissance Association Report No. GEER-040*. Version 1.1 August 7, 2015. doi:10.18118/G61591.

[2] Takai N, Shigefuji M, Rajaure S, Bijukchhen S, Ichiyanagi M, Dhital MR, and Sasatani T (2016): Strong ground motion in the Kathmandu Valley during the 2015 Gorkha, Nepal, Earthquake. *Earth Planets and Space* 68, 10, doi: 10.1186/s40623-016-0383-7.

[3] Stöcklin, J and Bhattarai, KD (1981): Geological map of Kathmandu area and central Mahabharat Range (1:250,000). Department of Mines and Geology, His Majesty Government of Nepal.

[4] Moribayashi S and Maruo Y (1980): Basement topography of the Kathmandu Valley, Nepal: An application of gravitational method to the survey of a tectonic basin in the Himalayas. *Journal of the Japan society of Engineering Geology*. 21-2.

[5] Cho I, Tada T, and Shinozaki Y (2006): Centerless circular array method: Inferring phase velocities of Rayleigh wave in broad wavelength range using microtremor records. *Journal of Geophysical Research* 111, B09315.

[6] Yokoi T (2005): Combination of Down Hill Simplex Algorithm with Very Fast Simulated Annealing Method-an Effective Cooling Schedule for Inversion of Surface Wave's Dispersion Curve. *Proc. of the Fall Meeting of Seismological Society of Japan*; B049.

[7] Wathelet M (2008): An improved neighborhood algorithm: Parameter conditions and dynamic scaling. *Geophysical Research Letters* 35, L09301, doi:10.1029/2008GL033256.

[8] Konno K, Suzuki T, Kamata Y, Nagao T (2007): Estimation of average S-wave velocity of ground using microtremors at strong-motion sites in Yokohama. *Journal of Japan Society of Civil Engineering* 63:639–654.

[9] Schnabel PB, Seed HB, and Lysmer J. (1972): SHAKE: A computer program for earthquake response analysis of horizontally layered sites. *Report No. UCB/EERC-72/12*; University of California, Berkeley, December, 102p.

